

Protected but Accessible: Oxygen Activation by a Calixarene-Stabilized Undecagold Cluster

Xi Chen[†] and Hannu Häkkinen^{*,†,‡}

[†]Department of Chemistry and [‡]Department of Physics, Nanoscience Center, University of Jyväskylä, FI-40014 Jyväskylä, Finland

S Supporting Information

ABSTRACT: DFT computations show that calixarenes stabilize subnanometer Au₁₁ clusters allowing access of small molecules like O₂ to reactive metal sites in the core. Maximum of three dioxygen molecules can bind to the cluster, and they are activated to a superoxo O₂⁻ state. This study predicts that gold clusters could act as viable oxidation catalysts at ambient conditions based on similar principles as the metal centers in enzymes.

Gold nanoparticle catalysts have been intensively studied for decades,¹ and the various factors inducing the catalytic activity and atomistic reaction mechanisms are still under active discussion.² Efficient aerobic oxidation under mild conditions is a particularly intriguing property of catalytically active nanoscale gold; hence, binding and activation of dioxygen is regarded as the crucial reaction step. It is generally agreed that control of size is crucial for keeping optimal dispersion (in many cases 2–3 nm) of gold on the support. Stabilizing the gold nanoparticles by organic ligands to prevent aggregation offers one alternative for controlling the size but raises new challenges for maintaining accessibility to reactive metal sites.³

Enzymes maintain unsaturated sites of the reactive metal centers in the presence of reaction inhibitors while facilitating access for reactants to the active sites.⁴ This highly selective action is accomplished since the protein backbone consists of a series of rigid segments that form a cage-like structure to surround each metal-cluster active site with an effective mesh size large enough to be penetrable to small reactant molecules. Similar function could be mimicked by suitable design of organic macrocycles or dendrimeric structures stabilizing gold nanoclusters.^{5,6}

Recently, de Silva et al. synthesized a group of calixarene-stabilized gold clusters using structurally defined ClAu(I)-diphosphine-calix[4]arene complexes as precursors.⁶ Although the total structure determination of the clusters could not be achieved, HAADF-STEM (high angle annular dark field-scanning tunneling electron microscopy) evidence suggested that the smallest clusters consist of a uniform distribution of subnanometer metal cores consisting of only 11 Au atoms, which was consistent with Au₁₁ cluster fragments that were observed via electron-spray-ionization (ESI) mass spectroscopy. Elemental analysis and X-ray photoelectron spectroscopy data were both consistent with binding of five calixarene phosphine ligands per Au₁₁ cluster, out of which two are bound in a bidentate fashion while three others are bound in monodentate fashion. Furthermore, steady-state fluorescence titration experi-

ments with probe molecule 2-naphthalenethiol (2NT) showed that 25% of the Au atoms in the metal core remain accessible and bind 2NT. The calix[4]arene ligand was thus shown to stabilize subnanometer gold clusters with accessible metal core sites for, e.g., adsorption and catalytic applications.

Inspired by this experiment and our earlier theoretical work on atomic and electronic structure of similar-size gold nanoclusters stabilized by phosphines, halides, and thiols,^{7,8} we performed density functional theory calculations on atomistic models based on the well-known undecagold Au₁₁ clusters^{7–9} and full diphosphine-calix[4]arene ligands used in the de Silva et al. experiment.⁶ We show here that binding of five calixarenes is sterically feasible and that three gold sites of the protected cluster have significant solvent accessibility. We further show that binding of 2NT or smaller molecules to accessible sites of the gold core is possible, and most importantly, we show that the calixarene-stabilized Au₁₁ cluster is able to simultaneously bind and activate up to three O₂ molecules to superoxo-like state, which predicts that these systems should be feasible for small-molecule oxidation reactions. In addition to providing strong support to the experiments of de Silva et al., our results validate one of the first computational models for ligand-stabilized subnanometer size gold clusters that could act as viable oxidation catalysts based on similar principles as for metal centers in enzymes.

We used the projector-augmented-wave (PAW) method in real space grids as implemented in the GPAW DFT code.¹⁰ The real space grid had a grid spacing of 0.2 Å. Au(5d¹⁰6s¹), P(3s²3p³), C(2s²2p²), O(2s²2p⁴) and H(1s¹) electrons were regarded as the valence. The PAW setup for Au includes scalar-relativistic corrections. We used PBE (Perdew-Burke-Ernzerhof)¹¹ as the exchange-correlation functional. All calculations were spin-polarized. All cluster systems were fully relaxed without any symmetry constraints until the residual forces were below 0.05 eV/Å. Electronic states in the metal core were analyzed by projection of the cluster states to spherical harmonics in a sphere of radius 4 Å as described in ref 7. VMD software (<http://www.ks.uiuc.edu/Research/vmd/>) was used to evaluate solvent-accessible surfaces and to visualize them.

First, we studied the geometric structure¹² of 1 Au₁₁L₅ and 2 Au₁₁L₅(2NT)₃ complexes where L = diphosphine calix[4]arene, see Figure 1. **1** consists of an Au₁₁ core which has an approximate C_{3v} symmetry, two bidentate bound ligands (Figure 1b), and three monodentate bound ligands (Figure

Received: June 14, 2013

Published: August 22, 2013

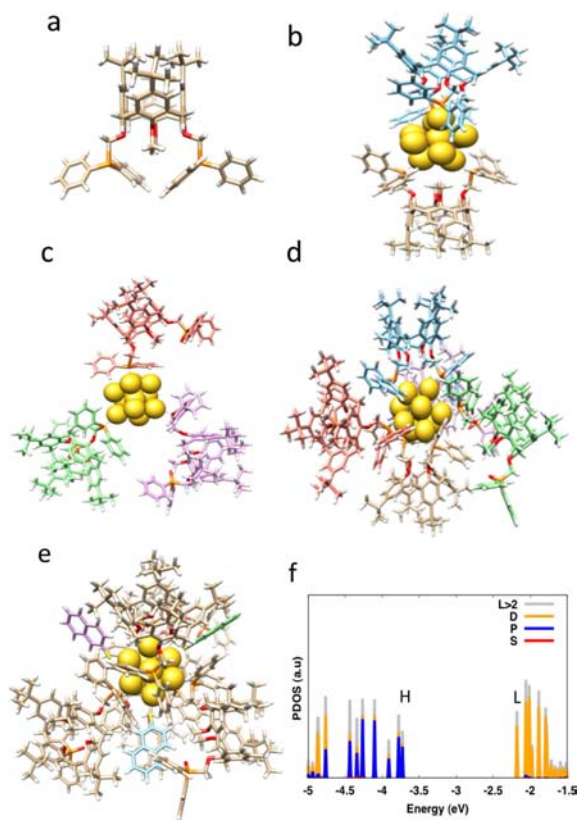


Figure 1. (a) Diphosphine-calixarene complex as determined by single-crystal X-ray diffraction (ref 6); (b) two bidentate ligands of Au_{11}L_5 ; (c) three monodentate ligands of Au_{11}L_5 ; (d) the full structure of $1 \text{ Au}_{11}\text{L}_5$ (the bidentate ligands are shown in light brown and light blue, while the monodentate ligands are in red, green, and purple); (e) the structure of $2 \text{ Au}_{11}\text{L}_5(2\text{NT})_3$ (all the calixarene ligands are shown in light brown and 2NT molecules are shown in purple, light blue, and green); (f) the angular-momentum projected density of states (PDOS) of $\text{Au}_{11}\text{L}_5(2\text{NT})_3$ in the Au_{11} core. H and L denote HOMO and LUMO, respectively. Note that several states close to the HOMO are due to 2NT ligands as well. The colors of the atoms: Au, yellow; P, orange; O, red; S, light yellow.

1c). The two bidentate ligands are on the opposite sides of the cluster and criss-cross with each other, while the monodentate ligands consist of bound phosphine and unbound phosphine-oxide substituents and bind to three C_{3v} symmetrical Au atoms. There are seven P–Au contacts to the metal core and the distances between Au and P atoms are $\sim 2.38 \text{ \AA}$, independent of the ligands being in monodentate or bidentate bound modes. Three Au sites (27% of metal sites) remain accessible to molecules as visualized by solvent-accessible surface of **1** shown in Figure 2.

The optimized structure of **2** is shown in Figure 1e. The three 2NT molecules bind to the three C_{3v} symmetrical Au sites with an average S–Au distance of 2.37 \AA , and the adsorption of 2NT molecules causes no major rearrangement of calixarene ligands. $\text{Au}_{11}\text{L}_5(2\text{NT})_3$ is stable not only because it has a high symmetry and is fully protected (all the Au atoms on the surface have a bond either with P or S atoms), but also because it has a special stable electronic structure which will be discussed in the following paragraph.

The ligand-protected gold clusters can be generally written with the formula $(\text{L}_x\text{Au}_N\text{X}_M)^z$ where N is the number of gold atoms in the cluster, L is an electron-neutral ligand (here the



Figure 2. Solvent-accessible surface of Au_{11}L_5 , showing one of the three Au sites available for binding reactants. Water molecule has been used as the probe. The accessible area at the three Au sites is $1.7\text{--}1.9 \text{ \AA}^2$.

phosphine-calixarene), M is the number of electron-withdrawing ligands X (here 2NT) and z is the charge in units of lel . The ‘metallic’ (delocalized, itinerant) electrons in the gold core can be counted by the simple formula⁷

$$n_e = N\nu_{\text{Au}} - M - z \quad (1)$$

where $\nu_{\text{Au}} = 1$ is the gold 6s valence number. For stable clusters, the electron counting from the eq 1 are those of well-known shell closing numbers $n_e = 2, 8, 18, 20, 34, 58, \dots$ ^{7,13} With the use of this electron counting rule, the neutral $\text{Au}_{11}\text{L}_5(2\text{NT})_3$ complex has 8 ‘metallic’ electrons in the gold core and the expected ‘superatom’ octet configuration of $1\text{S}^21\text{P}^6$ is confirmed by our analysis of spherical harmonics as visualized in Figure 1f. The figure shows that the cluster has a HOMO–LUMO gap of 1.55 eV . The HOMO state has the P symmetry and LUMO has the D symmetry. This calculation confirms that the electron counting rule works not only for the Au clusters with small and monodentate bound ligands, but also for the clusters with more bulky ligands, which are bound in both monodentate and bidentate fashions.

Previously, we discovered an interesting trend relating the electronic structure and reactivity for small phosphine-halide protected gold clusters.⁸ If an electron-withdrawing ligand of a fully protected cluster is replaced by O_2 , binding of the dioxygen is significant only for the small gold clusters, which have a large HOMO–LUMO gap. The considerable HOMO–LUMO gap of $\text{Au}_{11}\text{L}_5(2\text{NT})_3$ suggests that, if one lets O_2 instead of 2NT react with Au_{11}L_5 , the cluster will adsorb and activate O_2 .

To check our hypothesis, we first studied Au_{11}L_5 with one O_2 . The complex $3 \text{ Au}_{11}\text{L}_5\text{O}_2$ is shown in Figure 3a. The adsorption of O_2 hardly changes the positions of calixarene ligands. The length of Au–O bond is 2.14 \AA and the angle of Au–O–O is 120.9° . The binding energy of O_2 is 1.06 eV , and the O–O distance is 1.33 vs 1.24 \AA in the neutral triplet O_2 . To understand the interaction between the cluster and O_2 , we analyzed the electronic properties of Au_{11}L_5 and $\text{Au}_{11}\text{L}_5\text{O}_2$. For Au_{11}L_5 , there are 11 delocalized electrons in the Au_{11} core according to eq 1; therefore, the HOMO, HOMO-1, HOMO-2 states of the cluster all show the D symmetry corresponding to the $1\text{S}^21\text{P}^61\text{D}^3$ electronic states in the metal core. On the adsorption of one O_2 , the electronic states of the metal core shift. The spin-up HOMO-1 D state of Au_{11}L_5 depletes completely and the electron is transferred to one of the $2\pi^*$ orbitals of O_2 , which is empty in the gas-phase triplet O_2 (Figure 3c). Occupation of $2\pi^*$ orbital and stretch of the O–O bond length verifies that the dioxygen is activated to the

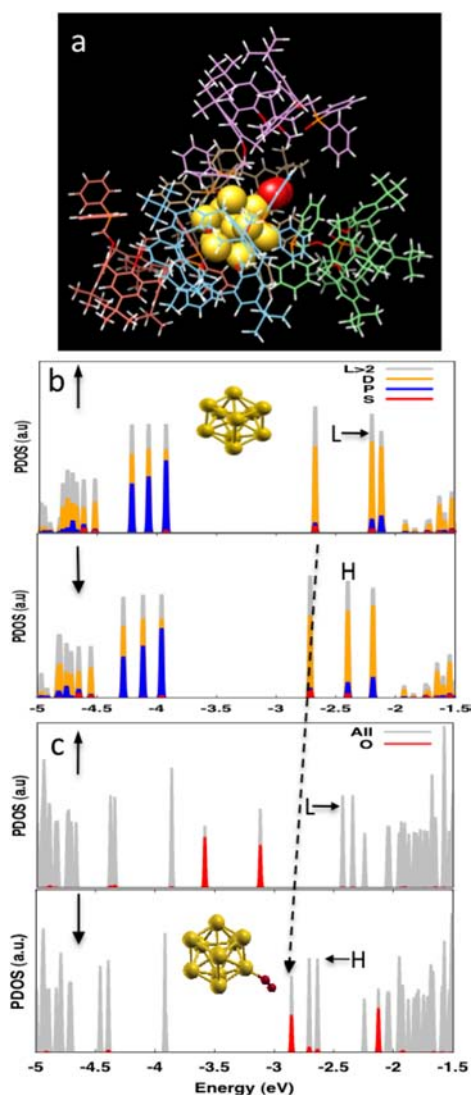


Figure 3. (a) The structure of 3 $\text{Au}_{11}\text{L}_5\text{O}_2$ complex; (b) the spindependent angular-momentum-projected density of states (PDOS) of Au_{11}L_5 cluster in the Au_{11} core; (c) the density of states of O_2 and $\text{Au}_{11}\text{L}_5\text{O}_2$. The insets show the relaxed structures of Au_{11}L_5 and $\text{Au}_{11}\text{L}_5\text{O}_2$ without showing the calixarene ligands. The O–O distance in the oxygen molecule is 1.33 Å. The colors of atoms and ligands are as in Figure 1.

superoxo-like O_2^- state. This result is in good agreement with the previous work.⁸

Au_{11}L_5 has three unsaturated Au sites, and three superatom electrons over the shell-closing count of 8. Consequently, it should be able to adsorb three O_2 molecules. The optimized structure of 4 $\text{Au}_{11}\text{L}_5(\text{O}_2)_3$ is shown in Figure 4a. Cluster 4 has C_{3v} symmetry and the adsorption of the O_2 molecules causes no obvious distortion for calixarene ligands. The average Au–O distance is 2.18 Å and the average Au–O–O angle is 120.5° . When Au_{11}L_5 adsorbs three O_2 , the spin-up HOMO-1 D orbital of Au_{11}L_5 depletes and the electron is transferred to the spin-up $2\pi^*$ orbital of one O_2 , while the spin-down HOMO and HOMO-2 D orbitals of Au_{11}L_5 deplete and the electrons are transferred to the degenerate spin-down $2\pi^*$ orbitals of other two O_2 (Figure 4c). The average O–O distance is 1.32 Å and the average bonding energy of O_2 is 1.02 eV per molecule; all these bonding characteristics are very similar to complex (3)

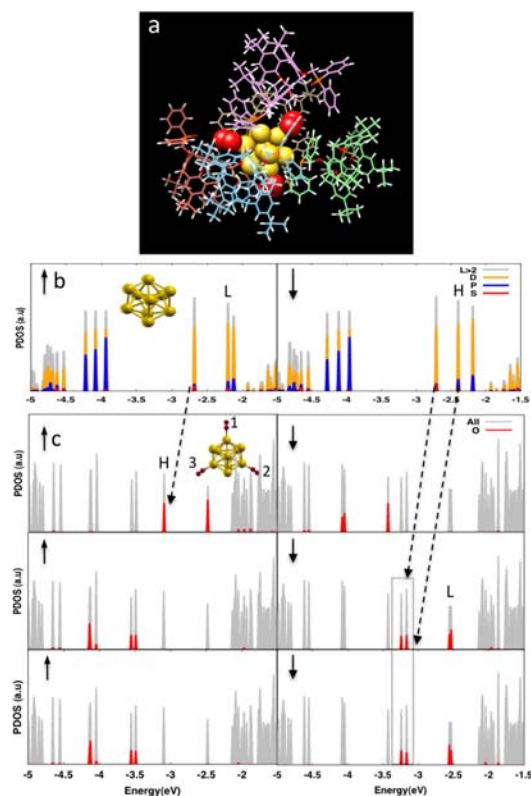


Figure 4. (a) The structure of 4 $\text{Au}_{11}\text{L}_5(\text{O}_2)_3$ complex; (b) the spin-dependent angular-momentum-projected density of states (PDOS) of Au_{11}L_5 cluster in the Au_{11} core; (c) PDOS of three O_2 (the three O_2 marked by 1, 2, 3 and their PDOS are shown from top to bottom in (c), respectively) in the $\text{Au}_{11}\text{L}_5(\text{O}_2)_3$. The insets show the relaxed structures of Au_{11}L_5 and $\text{Au}_{11}\text{L}_5(\text{O}_2)_3$ without showing the calixarene ligands. The average O–O distances are 1.32 Å in oxygen molecules 1, 2, and 3. The colors of atoms and ligands are as in Figure 1.

which shows that the three O_2 adsorption events to the three accessible gold sites are independent from each other.

In conclusion, we have validated that calixarenes can form a protective but porous ligand layer on the surface of a subnanometer Au_{11} cluster, while maintaining accessibility to metal sites of the core. Three out of 11 Au atoms (27%) remain accessible to small reactant molecules, and it was shown here that binding and activation of up to three dioxygen molecules per cluster can take place. Our computational results provide strong support for a recent experiment⁶ and predict that this class of stable hybrid metal–organic nanomaterial should be very interesting for catalyzing aerobic oxidation reactions at ambient conditions.

■ ASSOCIATED CONTENT

📄 Supporting Information

Full ref 10b, total energies and coordinates of structures 1–4. This material is available free of charge via the Internet at <http://pubs.acs.org>.

■ AUTHOR INFORMATION

Corresponding Author

hannu.j.hakkinen@jyu.fi

Notes

The authors declare no competing financial interest.

ACKNOWLEDGMENTS

This work was supported by the Academy of Finland. The computer resources were provided by CSC – the Finnish IT Center for Science. We thank A. Katz and K. Salorinne for useful correspondence.

REFERENCES

- (1) (a) Haruta, M. *Catal. Today* **1997**, *36*, 153. (b) Bond, G. C.; Thompson, D. *Catal. Rev.: Sci. Eng.* **1999**, *41*, 319. (c) Valden, M.; Lai, X.; Goodman, D. W. *Science* **1998**, *281*, 1647. (d) Meyer, R.; Lemire, C.; Shaikhutdinov, S.; Freund, H.-J. *Gold Bull.* **2004**, *37*, 72. (e) Hashmi, A. S. K.; Hutchings, G. J. *Angew. Chem., Int. Ed.* **2006**, *45*, 7896. (f) Corma, A.; Garcia, H. *Chem. Soc. Rev.* **2008**, *37*, 2096.
- (2) (a) Sanchez, A.; Abbet, S.; Heiz, U.; Schneider, W.-D.; Häkkinen, H.; Barnett, R. N.; Landman, U. *J. Phys. Chem. A* **1999**, *103*, 9573. (b) Häkkinen, H.; Abbet, S.; Sanchez, A.; Heiz, U.; Landman, U. *Angew. Chem., Int. Ed.* **2003**, *42*, 1297. (c) Yoon, B.; Häkkinen, H.; Landman, U.; Wörz, A.; Antonietti, J.-M.; Abbet, S.; Judai, K.; Heiz, U. *Science* **2005**, *307*, 403. (d) Lopez, N.; Janssens, T. V. W.; Clausen, B. S.; Xu, Y.; Mavrikakis, M.; Bligaard, T.; Nørskov, J. K. *J. Catal.* **2004**, *223*, 232. (e) Molina, L. M.; Hammer, B. *Phys. Rev. B* **2004**, *69*, 155424. (f) Laursen, S.; Linic, S. *Phys. Rev. Lett.* **2006**, *97*, 026101. (g) Falsig, H.; Hvolbæk, B.; Kristensen, I. S.; Jiang, T.; Bligaard, T.; Christensen, C. H.; Nørskov, J. K. *Angew. Chem., Int. Ed.* **2008**, *47*, 4835.
- (3) (a) Crooks, R. M.; Zhao, M.; Sun, L.; Chechik, V.; Yeung, L. K. *Acc. Chem. Res.* **2001**, *34*, 181. (b) Tsukuda, T. *Bull. Chem. Soc. Jpn.* **2012**, *85*, 151.
- (4) (a) Robbins, A. H.; Stout, C. D. *Proc. Natl. Acad. Sci. U.S.A.* **1989**, *86*, 3639. (b) Beinert, H. J. *Biol. Inorg. Chem.* **2000**, *5*, 2. (c) Banavar, J. R.; Maritan, A. *Annu. Rev. Biophys. Biomol. Struct.* **2007**, *36*, 261.
- (5) Tsunoyama, H.; Liu, Y. M.; Akita, T.; Ichikuni, N.; Sakurai, H.; Xie, S. H.; Tsukuda, T. *Catal. Surv. Asia* **2011**, *15*, 230.
- (6) de Silva, N.; Ha, J.-M.; Solovyov, A.; Nigra, M. M.; Ogino, I.; Yeh, S. W.; Durkin, K. A.; Katz, A. *Nat. Chem.* **2010**, *2*, 1062.
- (7) Walter, M.; Akola, J.; Lopez-Acevedo, O.; Jadzinsky, P. D.; Calero, G.; Ackerson, C. J.; Whetten, R. L.; Grönbeck, H.; Häkkinen, H. *Proc. Natl. Acad. Sci. U.S.A.* **2008**, *105*, 9157.
- (8) Lopez-Acevedo, O.; Kacprzak, K. A.; Akola, J.; Häkkinen, H. *Nat. Chem.* **2010**, *2*, 329.
- (9) (a) McPartlin, M.; Mason, R.; Malatesta, L. *Chem. Commun.* **1969**, 334. (b) Albano, V. G.; Bellon, P. L.; Manassero, M.; Sansoni, M. *Chem. Commun.* **1970**, 1210. (c) Bellon, P. L.; Manassero, M.; Sansoni, M. *J. Chem. Soc., Dalton Trans.* **1972**, 1481. (d) Bartlett, P. A.; Bauer, B.; Singer, S. J. *J. Am. Chem. Soc.* **1978**, *100*, 5085.
- (10) (a) Mortensen, J. J.; Hansen, L. B.; Jacobsen, K. W. *Phys. Rev. B* **2005**, *71*, 035109. (b) Enkovaara J. et al. *J. Phys.: Condens. Matter* **2010**, *22*, 253202. The code is available at: <https://wiki.fysik.dtu.dk/gpaw>.
- (11) Perdew, J. P.; Burke, K.; Ernzerhof, M. *Phys. Rev. Lett.* **1996**, *77*, 3.
- (12) The atomic coordinates of fully relaxed Au₁₁L₅, Au₁₁L₅(2NT)₃, Au₁₁L₅O₂, and Au₁₁L₅(O₂)₃ complexes are available from the corresponding author and also listed in the Supporting Information file.
- (13) (a) Akola, J.; Walter, M.; Whetten, R. L.; Häkkinen, H.; Grönbeck, H. *J. Am. Chem. Soc.* **2008**, *130*, 3756. (b) Aikens, C. M. *J. Phys. Chem. Lett.* **2011**, *2*, 99. (c) Häkkinen, H. *Chem. Soc. Rev.* **2008**, *37*, 1847.